Posted on 30 Jan 2024 — The copyright holder is the author/funder. All rights reserved. No reuse without permission. — https://doi.org/10.22541/au.170665457.70346859/v1 — This is a preprint and has not been peer-reviewed. Data may be preliminary.

In Vitro Measurement and In Vivo Prediction of Combination Safety of Rivaroxaban with Tyrosine Kinase Inhibitors: A Medication Safety Assessment Study

tingting Zhao[1], Xuening Li[1], Yanwei Chen[2], Dalong Wang[1], Liyan Wang[2], Shan Zhao[3], Changyuan Wang[1], Qiang Meng[1], Huijun Sun[1], Kexin Liu[1], and Jingjing Wu[1]

[1]Dalian Medical University
[2]First Affiliated Hospital of Dalian Medical University
[3]Chinese Academy of Sciences

March 07, 2024

Abstract

Background and Purpose: Rivaroxaban as an oral anticoagulant is widely used for the prevention and treatment of thromboembolic disease. Previous studies revealed cytochrome P450 (CYP)–mediated metabolism of rivaroxaban mainly involves CYP2J2 and CYP3A4. Imatinib, sunitinib and gefitinib are three tyrosine kinase inhibitors (TKIs) that are extensively applied for anti-cancer therapy. Statistical research has shown cancer patients are at approximately 4-7–fold higher risk of vein thromboembolism than normal patients. Therefore, rivaroxaban and TKIs have a profound combination foundation. This study aimed to comprehensively assess the combination safety of rivaroxaban with TKIs in vitro. Experimental Approach: First, the inhibitory activity of the three TKIs was screened. Second, to comprehensively evaluate their inhibitory potential, the reversible and mechanism-dependent inhibitory kinetic constants of three TKIs on CYP2J2 and CYP3A4 were determined. Docking simulation was used to explore the molecular mechanism. Finally, drug-drug interaction (DDI) risks of the combination were assessed using pharmacokinetic data of cancer patients. Key Results: Imatinib and gefitinib exerted significant reversible inhibition of both CYP2J2 and CYP3A4, while sunitinib only showed reversible inhibition of CYP3A4, not CYP2J2. Three TKIs also showed time-dependent inactivation of CYP3A4 and slightly on CYP2J2. Notably, sunitinib had a significantly stronger inactivation effect on CYP3A4 than the other TKIs, with a 4.14-fold IC50 shift. Imatinib was predicted to cause a 114–244% increase in rivaroxaban exposure. Conclusion and Implication: Imatinib showed the strongest inhibition, which was predicted to have a moderate DDI risk. These results provide evidence for medication guidance when combining rivaroxaban with TKIs.

In Vitro Measurement and In Vivo Prediction of Combination Safety of Rivaroxaban with Tyrosine Kinase Inhibitors: A Medication Safety Assessment Study

Tingting Zhao[a,b #], Xuening Li[a, b, #], Yanwei Chen[c, #], Dalong Wang[a], Liyan Wang[c], Shan Zhao[d], Changyuan Wang[a, b], Qiang Meng[a, b], Huijun Sun[a, b], Kexin Liu[a, b], Jingjing Wu[a, b*]

[a]Department of Clinical Pharmacology, College of Pharmacy, Dalian Medical University, Dalian 116044, China.

[b]Provincial Key Laboratory for Pharmacokinetics and Transport, Liaoning Dalian Medical University, Dalian, Liaoning, China.

[c]Department of Pharmacy, the First Affiliated Hospital of Dalian Medical University, Dalian 116011, China.

[d]Dalian Institute of Chemical Physics, Chinese Academy of Sciences, Dalian 116023, China.

Posted on 30 Jan 2024 — The copyright holder is the author/funder. All rights reserved. No reuse without permission. — https://doi.org/10.22541/au.170665457.70346859/v1 — This is a preprint and has not been peer-reviewed. Data may be preliminary.

# These authors contributed equally to this work.

*** Correspondence:**

Dr. Jingjing Wu

ORCID: 0000-0002-5046-9996

Department of Clinical Pharmacology, College of pharmacy

Dalian Medical University

9 West Section, Lvshun South Road, Lvshunkou District, Dalian 116044, China

Data availability statement

The data underlying this article will be shared on reasonable request to the corresponding author.

Funding

This work was supported by the National Natural Science Foundation of China (81874324, 81922070, 81973286, 81803627, 81702995 and U1608283), and LiaoNing Revitalization Talents Program (XLYC1907103).

Authors' Contributions

Tingting Zhao : Software, Validation, Formal analysis, Investigation, Writing-Original Draft. **Xuening Li** : Software, Validation, Formal analysis, Investigation, Writing Original Draft.**Yanwei Chen:** Software, Validation, Formal analysis, Investigation, Writing Original Draft. **Jingjing Wu** : Conceptualization, Supervision, Writing-review and editing.**Dalong Wang:** Supervision, Data Curation. **Shan Zhao** : Supervision, Data Curation. **Liyan Wang** : Supervision.**Changyuan Wang** : Project administration. **Qiang Meng** : Supervision. **Huijun Sun** : Supervision. **Kexin Liu** : Supervision.

Conflict of Interest

The authors declare that they have no conflict of interest.

Ethical Approval

This article does not contain any studies with human participants or animals performed by any of the authors.

Abstract

Background and Purpose: Rivaroxaban as an oral anticoagulant is widely used for the prevention and treatment of thromboembolic disease. Previous studies revealed cytochrome P450 (CYP)–mediated metabolism of rivaroxaban mainly involves CYP2J2 and CYP3A4. Imatinib, sunitinib and gefitinib are three tyrosine kinase inhibitors (TKIs) that are extensively applied for anti-cancer therapy. Statistical research has shown cancer patients are at approximately 4-7–fold higher risk of vein thromboembolism than normal patients. Therefore, rivaroxaban and TKIs have a profound combination foundation. This study aimed to comprehensively assess the combination safety of rivaroxaban with TKIs in vitro.

Experimental Approach: First, the inhibitory activity of the three TKIs was screened. Second, to comprehensively evaluate their inhibitory potential, the reversible and mechanism-dependent inhibitory kinetic constants of three TKIs on CYP2J2 and CYP3A4 were determined. Docking simulation was used to explore the molecular mechanism. Finally, drug-drug interaction (DDI) risks of the combination were assessed using pharmacokinetic data of cancer patients.

Key Results: Imatinib and gefitinib exerted significant reversible inhibition of both CYP2J2 and CYP3A4, while sunitinib only showed reversible inhibition of CYP3A4, not CYP2J2. Three TKIs also showed time-dependent inactivation of CYP3A4 and slightly on CYP2J2. Notably, sunitinib had a significantly stronger

Posted on 30 Jan 2024 — The copyright holder is the author/funder. All rights reserved. No reuse without permission. — https://doi.org/10.22541/au.170665457.70340859/v1 — This is a preprint and has not been peer-reviewed. Data may be preliminary.

inactivation effect on CYP3A4 than the other TKIs, with a 4.14-fold IC_{50} shift. Imatinib was predicted to cause a 114–244% increase in rivaroxaban exposure.

Conclusion and Implication: Imatinib showed the strongest inhibition, which was predicted to have a moderate DDI risk. These results provide evidence for medication guidance when combining rivaroxaban with TKIs.

Keywords: rivaroxaban, tyrosine kinase inhibitors, combined medication, CYP2J2, CYP3A4, drug-drug interaction, medication safe

Introduction

Rivaroxaban, an oral anticoagulant, is widely used for the prevention and treatment of thromboembolic disorders in clinical practice. It exhibits direct anticoagulant effects by inhibiting coagulation factor Xa. Although in vivo pharmacokinetic data are stable, bleeding is still a risk factor that be considered for medication safety. Our previous studies have shown CYP2J2 and CYP3A4 to be the major isoforms involved in the metabolic process of rivaroxaban, and importantly CYP2J2 showed ˜39-fold higher catalytic efficiency than CYP3A4 (Zhao et al., 2021). Notably, CYP2J2, which dominated the metabolism of rivaroxaban, is always not considered in routine drug-drug interaction (DDI) research due to its lower abundance in the liver. It is this lack of research that may lead to the possibility of severe rivaroxaban-related clinical DDIs being overlooked.

Cancer-related vein thromboembolism (VTE) is closely associated with increased morbidity and mortality (Song, Rosovsky, Connors & Al-Samkari, 2019). In cancer patients, the presence of tumours is one of the risk factors for VTE. Additionally, both the hypercoagulability of cancer patients and the thrombogenicity of anti-cancer agents are reasons for the high incidence of VTE in cancer patients (Shalhoub et al., 2017; Zamorano et al., 2016). According to statistics, cancer patients have an approximately 4–7-fold higher risk of VTE than normal patients, and cancer patients with VTE account for about 20% of all VTE patients (Blom, Doggen, Osanto & Rosendaal, 2005; Streiff, 2016). Meanwhile, thrombotic diseases are the leading cause of non-neoplastic death in cancer patients (Song, Rosovsky, Connors & Al-Samkari, 2019; Timp, Braekkan, Versteeg & Cannegieter, 2013; Zamorano et al., 2016). Therefore, coagulation prevention or anticoagulant treatment is unavoidable in cancer patients.

For decades, anticoagulant therapy for cancer-related VTE has been limited to vitamin K antagonists (VKAs) and heparin drugs. Recently, direct oral anticoagulants (DOACs) have also become an option (Streiff et al., 2020). Rivaroxaban is recommended for the treatment of superficial vein thrombosis and VTE prophylaxis following the discharge by the National Comprehensive Cancer Network of America in 2020 of the clinical practice guidelines for cancer-associated venous thromboembolic disease (Streiff et al., 2020). Similarly, the Chinese Society of Clinical Orology has also added rivaroxaban as a recommended anticoagulant for partial tumour patients. Additionally, data from large randomised clinical trials also suggest that DOCAs combined with validated risk assessment scores are a reasonable choice for the primary thromboprophylaxis of cancer patients instead of low molecular weight heparin (Song, Rosovsky, Connors & Al-Samkari, 2019). Importantly, Prins et al. found that rivaroxaban is similar to the standard treatment in terms of efficacy and safety for cancer patients, and the ease of taking this medicine improves patient adherence, and thus it may be used as an alternative to the standard therapy for some cancer patients (Prins et al., 2013; Sanfilippo & Wang, 2019).

In addition to the cautious selection of anticoagulation medication to achieve the best therapy outcomes, anticoagulant adverse effects can also be severe and alarming, which should be comprehensively prevented. Compared with non-cancer patients, the recurrence rate of VTE in cancer patients is 3–4 times higher and the incidence of major bleeding is also increased by 2–3 times (Douketis, Crowther, Foster & Ginsberg, 2001; Levitan et al., 1999; Monreal et al., 2006; Prandoni et al., 2002). In addition to VTE, the risk of atrial fibrillation (AF) for cancer patients was also extremely high (Onaitis, D'Amico, Zhao, O'Brien & Harpole, 2010). An analysis showed that the occurrence of AF for cancer patients in the 90 days after the cancer diagnosis was much higher than for normal patients (Saliba, Rennert, Gronich, Gruber & Rennert, 2018).

Posted on 30 Jan 2024 — The copyright holder is the author/funder. All rights reserved. No reuse without permission. — https://doi.org/10.22541/au.170665457.70340859/v1 — This is a preprint and has not been peer-reviewed. Data may be preliminary.

And, notably, there is growing awareness that many cancer-related factors are associated with AF, such as inflammations, metabolic or electrolyte abnormalities and cancer therapy (Crusz & Balkwill, 2015; Diakos, Charles, McMillan & Clarke, 2014; Farmakis, Parissis & Filippatos, 2014; Nattel, Burstein & Dobrev, 2008; Nattel & Harada, 2014). The prevention of stroke and systemic embolism by using anticoagulants is one of the therapeutic cornerstones of AF management (January et al., 2019). Therefore, cancer patients may receive anticoagulant therapy concurrently with anti-cancer therapy.

Tyrosine kinase inhibitors (TKIs) are a class of drugs that reduce the phosphorylation of tyrosine protein kinases. TKIs compete with tyrosine protein kinases for ATP phosphorylation sites to achieve targeted anti-tumour therapy (Jiao, Bi, Ren, Song, Wang & Wang, 2018). Among these, imatinib, sunitinib and gefitinib have been the mainstay treatments for various solid tumours and malignant blood diseases since their launch in 2000 (Burotto, Manasanch, Wilkerson & Fojo, 2015; Cheng et al., 2013; Kuczynski, Lee, Man, Chen & Kerbel, 2015; Tirumani, Jagannathan, Krajewski, Shinagare, Jacene & Ramaiya, 2013; Wertheimer et al., 2015). Imatinib was almost the first TKI anti-tumour drug to gain approval by the US Food and Drug Administration (FDA) and has become a first-line clinical drug for gastrointestinal stromal tumours (GIST) and chronic myeloid leukaemia (CLM) (O'Brien et al., 2003; von Mehren & Widmer, 2011). However, due to the long treatment cycles, the safety of imatinib in combination with other drugs is particularly important (Guilhot, 2004; Nebot, Crettol, d'Esposito, Tattam, Hibbs & Murray, 2010). As a multitargeted TKI, sunitinib exerts strong angiogenesis inhibitory activity. It was approved by the FDA in 2006 as a first-line drug for metastatic renal cell carcinoma, and it was also used as a second-line drug for imatinib-resistant patients (Kalra, Rini & Jonasch, 2015). Gefitinib was the first TKI to gain approval in the US and Japan for treating advanced non-small-cell lung cancer (NSCLC), and can significantly prolong the progression-free survival of NSCLC patients (Dhillon, 2015). It is noteworthy that CYP3A4 accounts for a considerable proportion of the CYP-mediated metabolism of these three TKIs, which is similar to rivaroxaban. Indeed, it is the overlap between the metabolic enzymes for rivaroxaban and these three TKIs that may produce DDIs.

The status of CYP2J2 in DDI evaluation is very different to that of CYP3A4, which may relate to the distribution characteristics of CYP2J2. CYP2J2 is a P450 isoform that is mainly distributed in the heart and arteries and is responsible for the metabolism of arachidonic acid; its expression is lower in the liver. However, CYP2J2 was recently highlighted as an emerging tumour marker. Numerous studies have reported the high expression of CYP2J2 in various cancer cell lines, tumour tissues and even in the liver of cancer patients, which may relate to tumour expansion and metastasis (Allison et al., 2017; Karkhanis, Hong & Chan, 2017). Therefore, inhibiting CYP2J2 may be a novel and effective approach for cancer therapy (Allison et al., 2017). However, safety assessment data on medication combinations are lacking, so the related roles of CYP2J2 are unknown.

Imatinib, sunitinib and gefitinib have been widely applied for patients with solid tumours in clinical practice. Thus, the comitant administration of rivaroxaban with these three TKIs has a profound combination foundation in the treatment of cancer patients. However, the safety of this combination deserves further attention as assessment data on the safety of rivaroxaban with TKIs is limited: more relevant and detailed pharmacokinetics measurements are required. The present study assessed the DDI risk of the combination of rivaroxaban with the three TKIs by in vitro enzyme assays. Importantly, the investigation was mainly performed on CYP2J2 and CYP3A4 to comprehensively explore their reversible and time-dependent inactivation behaviours. Finally, the in vivo DDI risk of the combination of rivaroxaban with the three TKIs was estimated according to detailed pharmacokinetic parameters of cancer patients, producing direct evidence to inform clinical medication safety assessment.

Posted on 30 Jan 2024 — The copyright holder is the author/funder. All rights reserved. No reuse without permission. — https://doi.org/10.22541/au.170665457.70340859/v1 — This is a preprint and has not been peer-reviewed. Data may be preliminary.

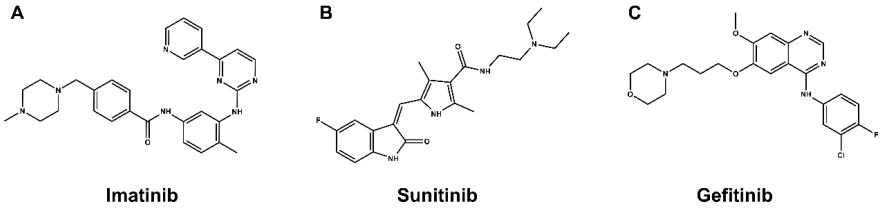

Figure. 1 Molecular structure of (A) imatinib, (B) sunitinib and (C) gefitinib.

Materials and methods

Materials and chemicals

Rivaroxaban, sunitinib and NADPH were purchased from Shanghai Yuanye Bio-Technology Co., Ltd. Imatinib and gefitinib were obtained from Sigma-Aldrich (Missouri, USA). cDNA-expressed recombinant human CYP3A4 was purchased from Cypex Ltd (Dundee, UK). Pooled human liver microsomes (HLM) and recombinant human CYP2J2 were purchased from BioreclamationIVT (Maryland, USA). The pooled HLM and recombined P450 isoforms were stored at –80 before experimentation. PBS was prepared from dipotassium bisulphate and potassium dihydrogen sulphate in the appropriate proportions and stored at 4 until use. All analytical reagent grade and HPLC grade solvents were from Tedia, Inc. (Ohio, USA).

High-performance liquid chromatography (HPLC) was performed using an Agilent MSD/MS system controller, two 1260 series pumps, a 1200 series autosampler and a 1200 series variable wavelength detector. Other instrumentation included a constant temperature vibrating mixer (Hangzhou ALLSHENG Instrument Co. Ltd, China), scroll machine, centrifuge and elite ODS-BP analysis column (4.6 × 200 mm, 5 μm).

Analytical methods

The inhibitory effect of the TKIs on the metabolism of rivaroxaban in recombined P450 isoforms and pooled human liver microsomes were compared by quantifiably detecting the production of the major metabolite using HPLC. The mobile phase consisted of 60% methanol (A pump) and 40% pure water with 0.2% formic acid (B pump) with isocratic elution. Detection conditions were as follows: column temperature, 30 °C; autosampler injection volume, 20 μL; flow rate, 0.5 mL·min^{-1}; and, detector wavelength, 240 nm. The amount of major rivaroxaban metabolite (M1) was determined from the rivaroxaban standard curve, for which the correlation coefficient was > 0.999.

Enzyme inhibition assays

The total volume of the incubation system with HLM was 200 μL, which contained rivaroxaban (200 μM), HLM (0.3 mg·mL^{-1}), TKIs, NADPH (10 mM final) and PBS. The total volume of the incubation system with recombined P450 isoforms was 100 μL, which contained rivaroxaban (400 μM), recombined enzymes (CYP2J2 0.4 mg·mL^{-1}, CYP3A4 0.6 mg·ml^{-1}), TKIs, NADPH (10 mM final) and PBS. The selection of the rivaroxaban concentration depended on the K_m values of the kinetic studies (22.81, 19.37 and 46.98 μM for HLM, CYP2J2 and CYP3A4, respectively), as reported in our previous study (Zhao et al., 2021). The concentration of CYP3A4 (0.6 mg·mL^{-1}) was selected to correspond with the lowest detected concentration of M1. The detailed method can be found in our previous publication (Zhao et al., 2021). Briefly, rivaroxaban, TKIs, enzymes and PBS were pre-incubated at 37 for 5 min, following which NADPH was added to initiate the reaction. After 60 min, the reaction was terminated by adding an equal volume of ice-cold methanol. The samples were centrifuged at 2000 x g for 15 minutes at 4 . Aliquots of the supernatants were stored at –20 degC until analysis by HPLC.

Reversible inhibition of CYP3A4 and CYP2J2 by TIKs

Rivaroxaban was used as the probe substrate for the determination of reversible inhibition kinetics values. The incubation system with CYP3A4 included rivaroxaban (0–400 μM), potential inhibitor (imatinib: 0–10 μM; gefitinib: 0–10 μM; sunitinib: 0–20 μM), NADPH and PBS. The incubation system with CYP2J2

Posted on 30 Jan 2024 — The copyright holder is the author/funder. All rights reserved. No reuse without permission. — https://doi.org/10.22541/au.170665457.70346859/v1 — This is a preprint and has not been peer-reviewed. Data may be preliminary.

included rivaroxaban (0–100 μM), potential inhibitor (imatinib, gefitinib and sunitinib), NADPH and PBS. The inhibition constant (K_i) was determined using various concentrations of inhibitors and rivaroxaban. $K_i$was calculated by three inhibition mode formulae (competitive, non-competitive and mixed-mode) using Prism v.6.0 (GraphPad, San Diego, CA, USA). Detailed information on the fitting formulae and related parameters can be found in our previous publication (Li, Cao, He, Ge, Guo & Wu, 2018).

IC_{50}shift assay

The 30 min pre-incubation of TKIs with NADPH and CYP2J2 preceded the normal incubation, following which the IC_{50} values (IC_{50} shift) were re-determined. These IC_{50} shift values were compared with the IC_{50} values that were determined without the 30 min pre-incubation, with a more than 1.5-fold decrease considered to be evidence of time-dependent inactivation. Other reaction conditions were as mentioned above.

Time-dependent inactivation of CYP3A4

To investigate the time-dependent inactivation of CYP3A4 by sunitinib, seven gradient concentrations (0–5 μM) and six time points (0–20 min) were used. It is worth noting that a higher substrate concentration than its Michaelis-Menten constant is required to reduce reversible inhibition. The data were then fitted to a linear regression model, which reflected the linear relation between 'ln remaining activity' and 'inactivation concentration' (I). The negative slope of this linear relationship reflected the observed inactivation rates (K_{obs}) value, which could be plotted against I to allow the fitting of inactivation kinetic parameters$K_{\ I}$ and $K_{\ \text{inact}}$ to the nonlinear least-squares regression based on Eq. 1. Using Prism v.6.0 (GraphPad, San Diego, CA, USA).

(1)

Molecular docking simulations

The CYP2J2 crystal structure homology model was used to conduct molecular docking simulations between TKIs and rivaroxaban in SYBYL (X-1.1). The CYP2J2 model was constructed using the Clustal Omega webserver (https://www.ebi.ac.uk/Tools/msa/clustalo/), as previously described (Ning et al., 2019). The crystal structure of CYP3A4 (PDB: 4D7D) was from the crystal structures that bound to a known inhibitor. The 3D structures of the TKIs were subjected to energy minimisation using the default Tripos force field parameters, and the Gasteiger-Hückel charges were calculated for each compound. The Surflex-Dock mode was used to generate binding conformations of TKIs with CYP2J2, from which the optimal conformations were determined by their empirical functions ChemScore. The PyMOL Molecular Graphics System v.16.1.0.15350 (DeLano Scientific LLC) was used to visualise the docking results.

Quantitative prediction of DDI risk

Kinetic constants were included in the mechanistic static model to explore reversible inhibition and time-dependent inactivation. This static model was previously developed and refined by Fahmi et al. (Fahmi, Maurer, Kish, Cardenas, Boldt & Nettleton, 2008) and Isoherranen et al. (Isoherranen, Lutz, Chung, Hachad, Levy & Ragueneau-Majlessi, 2012) to account for the inhibition of multiple P450 isoforms. In the present study, this model was designed to explore the contributions of enzyme inhibition in the prediction of DDI risk. The area under the curve ratio (AUCR) in the presence of a pharmacokinetic DDI was used as the index, as described by Eq. 2.

(2)

Here, A is the time-dependent inactivation of each P450 isoform that was observed in the liver, as described by Eq. 3.

(3)(4)

Here, B is the reversible inhibition of each P450 isoform that was observed in the liver, as described by Eq. 4. The degradation rates (K_{deg}) of CYP2J2 and CYP3A4 were 0.00026 and 0.00032 min^{-1}, respectively

Posted on 30 Jan 2024 — The copyright holder is the author/funder. All rights reserved. No reuse without permission. — https://doi.org/10.22541/au.170665457.70346859/v1 — This is a preprint and has not been peer-reviewed. Data may be preliminary.

(Cheong et al., 2017), where I represented the in vivo concentration of inhibitors in healthy and solid tumour patients. Additionally, the fraction of rivaroxaban metabolised by CYP2J2 or CYP3A4 was input from our previous study (Zhao et al., 2021), which were 0.95 for CYP2J2 and 0.025 for CYP3A4.

Results

Initial screening of TKI inhibitory activity

The inhibitory effects of the three TKIs, imatinib, sunitinib and gefitinib, on rivaroxaban metabolism with HLM, CYP3A4 and CYP2J2 were initially investigated at three TKI concentrations (1, 10, and 100 μM). Generally, imatinib and gefitinib showed strong inhibition of the metabolism of rivaroxaban, but sunitinib only exerted inhibitory activity in the incubation with HLM and CYP3A4. As shown in Figure 2A, imatinib had the most potent inhibitory effect on rivaroxaban metabolism with HLM, inhibiting approximately 50% of catalytic activity at 1 μM. Imatinib also showed the strongest inhibitory effect on CYP3A4-mediated rivaroxaban metabolism, with undetectable formation of M1 in the incubation with 100 μM imatinib (Figure 2B). Imatinib and gefitinib showed similar inhibition at 1 and 10 μM towards the metabolism mediated by CYP2J2 (Figure 2C). While sunitinib had minimal inhibitory effect on the metabolism of rivaroxaban by CYP2J2, the residual enzyme activity was more than 70% at 100 μM (Figure 2C).

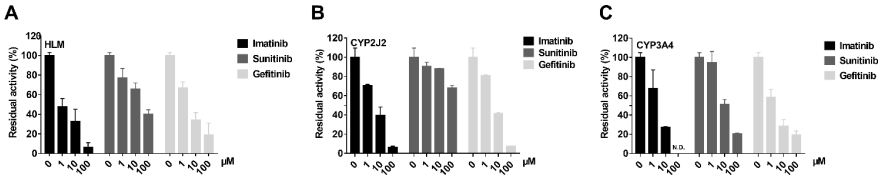

Figure 2. The initial screening of imatinib, sunitinib and gefitinib inhibition with: (A) HLM, (B) CYP2J2 and (C) CYP3A4. The TKI concentrations were 1, 10 and 100 μM. Results are shown as the mean ± S.D. of at least three determinations. N.D.: not detectable.

Determination of IC_{50} values

The concentration range was determined according to the results obtained from the initial screening. Both imatinib and gefitinib showed a strong inhibitory effect on the rivaroxaban metabolism mediated by CYP3A4 and CYP2J2, with IC_{50} values below 10 μM (Figure 3B, C and Table 1). Additionally, sunitinib exerted a potent inhibitory effect against CYP3A4-mediated metabolism, while the effect on CYP2J2-mediated metabolism was not obvious with an IC_{50} value of 397.70 μM (Figure 3E, F). Notably, in CYP3A4-mediated rivaroxaban metabolism, imatinib showed the strongest inhibitory activity with an IC_{50} value of 4.57 μM, while gefitinib showed the strongest inhibitory effect on metabolism by CYP2J2 with an IC_{50} value of 3.71 μM. In the metabolism associated with HLM incubation, imatinib was also the strongest inhibitor of the three TKIs with an IC_{50} of 1.69 μM (Figure 3A). The detailed IC_{50} values are shown in Table 1.

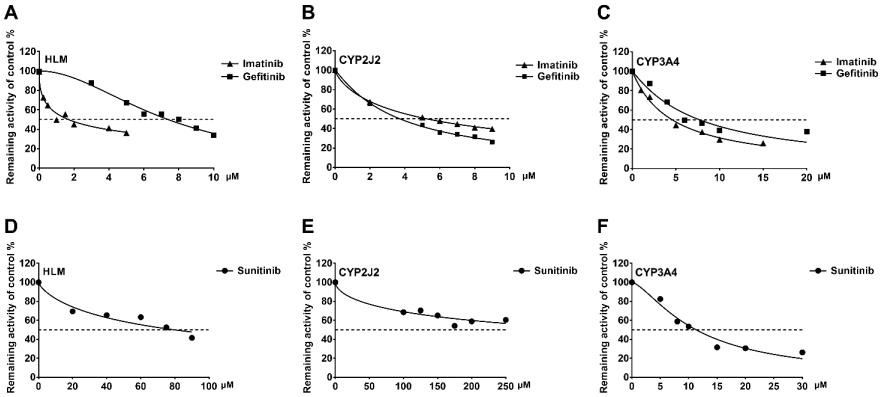

Posted on 30 Jan 2024 — The copyright holder is the author/funder. All rights reserved. No reuse without permission. — https://doi.org/10.22541/au.170665457.70340859/v1 — This is a preprint and has not been peer-reviewed. Data may be preliminary.

Figure 3 Dose-response curves of TKI inhibition with (A, D) HLM, (B, E) CYP2J2 and (C, F) CYP3A4. Results are shown as the mean from at least three experiments.

Table 1. IC_{50} values of TKI inhibition of rivaroxaban metabolism.

TKI	HLM	CYP2J2	CYP3A4
Imatinib	1.69 ± 0.130	5.23 ± 0.0777	4.57 ± 0.234
Sunitinib	79.56 ± 7.01	397.70 ± 105	11.30 ± 0.561
Gefitinib	7.39 ± 0.203	3.71 ± 0.131	7.72 ± 0.492

Data are reported as μM and were obtained from three independent experiments. All data represent the mean ± S.D.

Reversible inhibition behaviour of TKIs on CYP3A4 and CYP2J2

The reversible inhibition of CYP3A4 and CYP2J2 was investigated with various concentrations of rivaroxaban in the presence and absence of the TKIs (Figures 4, 5). The concentrations of rivaroxaban covered the $1/5K_m$–$5K_m$ range and the TKI concentrations covered the IC_{50} values. The K_i value of the TKIs was fitted from the kinetic curve and the R^2 values and inhibition modes are shown in Tables 2 and 3. As sunitinib did not exert more than 50% inhibition even at 250 μM, the K_i value was not measured. All three TKIs showed non-competitive inhibition on CYP3A4- and CYP2J2-mediated rivaroxaban metabolism with good correlation. This was corroborated by the respective Dixon and Lineweaver–Burk plots, which also showed that the TKIs inhibited rivaroxaban in the non-competitive mode. As with the IC_{50} results, imatinib showed the strongest inhibition on CYP3A4-mediated rivaroxaban metabolism with a K_i value of 1.92 μM. The K_i values of sunitinib and gefitinib with CYP3A4 were 13.24 and 4.91 μM, respectively, which were similar to their IC_{50} values. Imatinib and gefitinib showed similar inhibitory effects on CYP2J2, with K_i values of 3.53 and 2.99 μM, respectively. The detailed parameters are given in Tables 1 and 2.

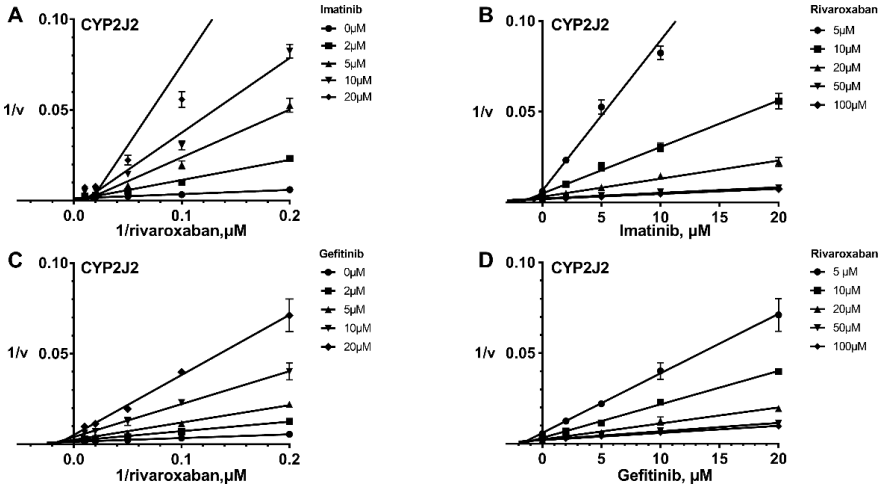

Figure 4. Reversible inhibition of CYP2J2 by imatinib and gefitinib. Lineweaver–Burk plots for the inhibition of (A) imatinib and (C) gefitinib (C) on CYP2J2-mediated rivaroxaban metabolism; (B) and (D) are the corresponding Dixon plots. The data represent the mean ± S.D. of triplicate experiments.

Posted on 30 Jan 2024 — The copyright holder is the author/funder. All rights reserved. No reuse without permission. — https://doi.org/10.22541/au.170665457.70346859/v1 — This is a preprint and has not been peer-reviewed. Data may be preliminary.

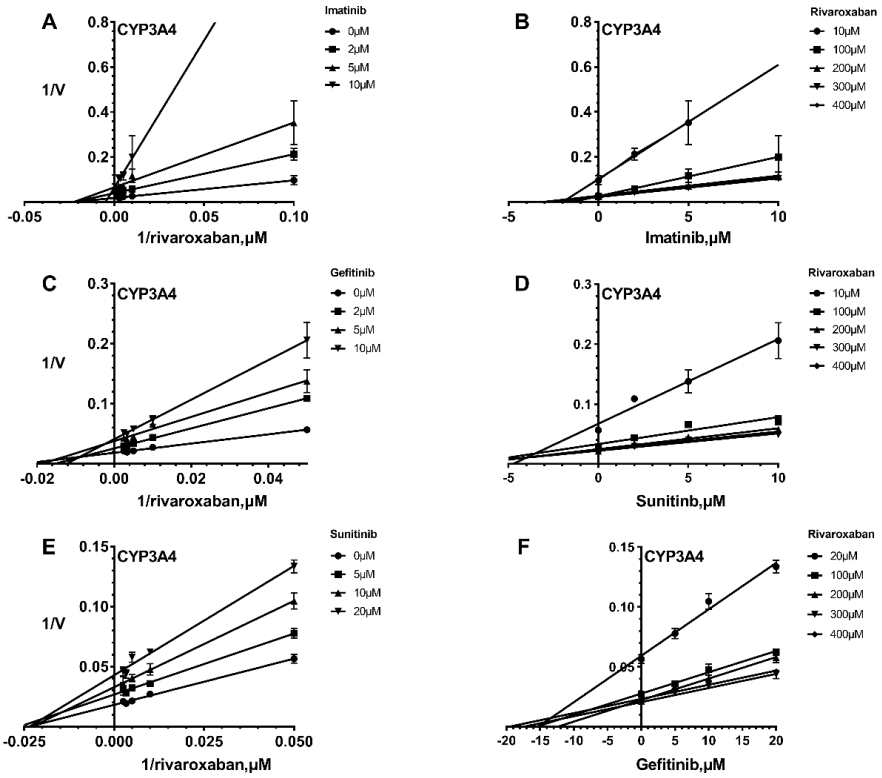

Figure 5. Reversible inhibition of CYP3A4 by imatinib, gefitinib and sunitinib. Lineweaver–Burk plots for the inhibition of (A) imatinib, (C) gefitinib and (E) sunitinib on CYP3A4-mediated rivaroxaban metabolism; (B), (D) and (F) are the corresponding Dixon plots. The data represent the mean ± S.D. of triplicate experiments.

Table 2. Reversible inhibition kinetic parameters for rivaroxaban metabolism mediated by CYP2J2.

TKI	$K_ι$ (μM)	Type	R^2
Imatinib	3.53 ± 0.221	Non-competitive	0.9514
Sunitinib	N.D.	N.D.	N.D.
Gefitinib	2.99 ± 0.123	Non-competitive	0.9784

The data are reported as the mean ± S.D. of three incubations. N.D.: not detectable.

Table 3. Reversible inhibition kinetic parameters of TKIs on rivaroxaban metabolism mediated by CYP3A4.

TKI	$K_ι$ (μM)	Type	R^2
Imatinib	1.92 ± 0.779	Non-competitive	0.9795
Sunitinib	13.24 ± 0.756	Non–competitive	0.9581
Gefitinib	4.91 ± 0.254	Noncompetitive	0.9562

The data are reported as the mean ± S.D. of three incubations.

IC_{50}-shift assays on CYP2J2 and CYP3A4

Posted on 30 Jan 2024 — The copyright holder is the author/funder. All rights reserved. No reuse without permission. — https://doi.org/10.22541/au.170665457.70346859/v1 — This is a preprint and has not been peer-reviewed. Data may be preliminary.

To comprehensively explore the inhibitory effects of the TKIs on the two P450 isoforms, their mechanism-dependent inhibition was investigated. IC_{50} shift assays of CYP2J2 and CYP3A4 were performed. Compared with direct inhibition (IC_{50}: 5.23 and 3.71 μM for imatinib and gefitinib, respectively), the 30-min pre-incubation with NADPH in the CYP2J2 incubation did not significantly change the inhibitory effect of imatinib and gefitinib (Figure 6A, C, and Table 4), while the inhibitory effect of sunitinib was slightly increased after the 30-min pre-incubation with NADPH in the CYP2J2 incubation with the IC_{50} decreasing 1.27-fold (Figure 6B and Table 4). Although the 30-min pre-incubation slightly increased its inhibitory activity, the inhibition of CYP2J2 by sunitinib was still weaker than by imatinib and gefitinib, with an IC_{50} of 312.90 μM (Table 4). In brief, the 30-min pre-incubation did not significantly affect the inhibition of CYP2J2 by the three TKIs, with all IC_{50}shifts being less than 1.5-fold. Additionally, all IC_{50}values for the inhibition of CYP3A4 by the TKIs decreased by more than 1.5-fold, which indicated that time-dependent inactivation of CYP3A4 by all three TKIs had occurred (Table 5.). Notably, sunitinib showed the largest change in IC_{50} shift (Figure 6E), with an IC_{50} value following the 30 min pre-incubation of 2.73 μM.

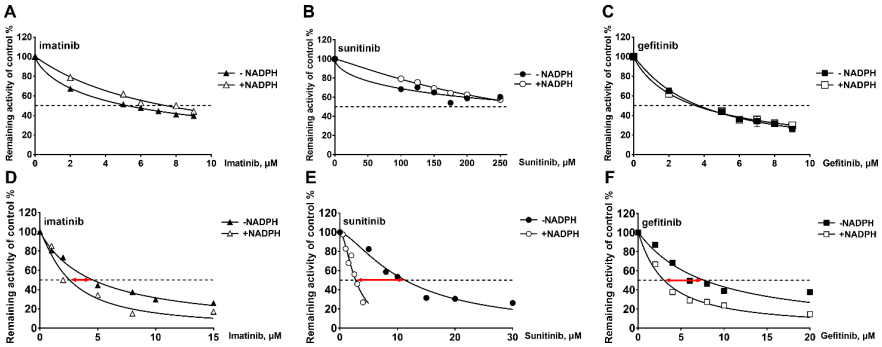

Figure 6. Effects of imatinib, sunitinib and gefitinib on rivaroxaban metabolism by (A, B and C) CYP2J2 and (D, E and F) CYP3A4 with or without a 30-min pre-incubation in the presence of NADPH. Data points are from three independent experiments.

Table 4. IC_{50} shifts initiated by pre-incubation of the three TKIs with NADPH in CYP2J2 incubations.

TKI	I˜$_{50}$ (μM)	IC_{50}-shift	Fold decrease
Imatinib	5.23 ± 0.0777	7.43 ± 0.208	0.70
Sunitinib	397.70 ± 105	312.90 ± 9.93	1.27
Gefitinib	3.71 ± 0.131	3.51 ± 0.0930	1.06

Data are reported as the mean ± S.D. of three incubations.

Table 5.IC_{50} shifts initiated by pre-incubation of the three TKI drugs with NADPH in CYP3A4 incubations.

TKI	I˜$_{50}$ (μM)	IC_{50}-shift	Fold decrease
Imatinib	4.57 ± 0.234	2.55 ± 0.370	1.79
Sunitinib	11.30 ± 0.5606	2.73 ± 0.149	4.14
Gefitinib	7.72 ± 0.492	3.03 ± 0.218	2.55

Data are reported as the mean ± S.D. of three incubations.

Time-dependent inactivation of CYP3A4 by sunitinib

Posted on 30 Jan 2024 — The copyright holder is the author/funder. All rights reserved. No reuse without permission. — https://doi.org/10.22541/au.170665457.70346859/v1 — This is a preprint and has not been peer-reviewed. Data may be preliminary.

Given the 4.14-fold IC_{50} shift of sunitinib on CYP3A4 following pre-incubation with NADPH for 30 min, various concentrations and pre-incubation times were used to determine the time-dependent inactivation constants (Figure 7A). The maximum inactivation rate (K_{inact}) and the inhibitor concentration needed to cause half of K_{inact} (K_I) were fitted using the non-linear regression method. As shown in Figure 7B, the K_{inact} and K_I values of sunitinib were 0.0339 min^{-1} and 2.901 μM, respectively. The K_{inact} value indicated that approximately 3.4% of CYP3A4 was inactivated per minute when it was incubated with the saturating concentration of sunitinib.

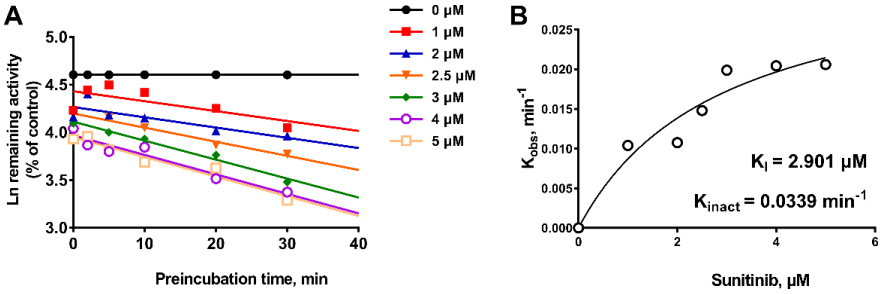

Figure 7. (A) Time- and concentration-dependent inactivation by sunitinib of CYP3A4-mediated rivaroxaban metabolism. (B) Observed inactivation rates (K_{obs}) were plotted against the sunitinib concentration to calculate the inactivation kinetic constants K_I and K_{inact} . Each point in Figure 7A was obtained from duplicate experiments.

Molecular docking simulations

Molecular docking simulations were used to elucidate the binding conformations for the interactions between the TKIs and CYP2J2 or CYP3A4. The corresponding ChemScore values of three TKIs are shown in Figure. 8. In the docking simulation between CYP2J2 and the TKIs, gefitinib had the lowest ChemScore value, followed by imatinib and then sunitinib. This ChemScore ranking was consistent with the inhibitory intensity of the TKIs on CYP2J2. Additionally, imatinib had the lowest ChemScore value in the docking simulation with CYP3A4, followed by gefitinib and then sunitinib, which was also consistent with the inhibitory intensity of these TKIs on CYP3A4.

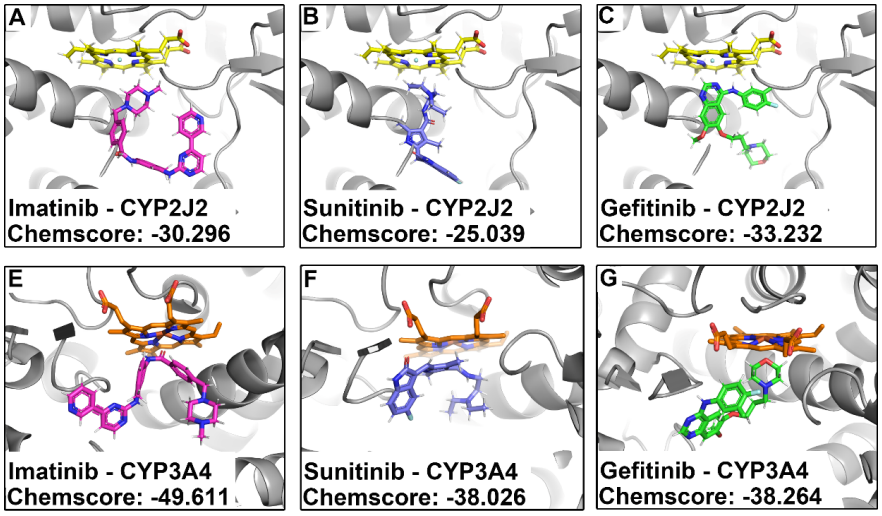

Figure 8. Molecular docking simulations of imatinib (A), sunitinib (B) and gefitinib (C) with CYP2J2, and (D, E and F) with CYP3A4.

Posted on 30 Jan 2024 — The copyright holder is the author/funder. All rights reserved. No reuse without permission. — https://doi.org/10.22541/au.170665457.70346859/v1 — This is a preprint and has not been peer-reviewed. Data may be preliminary.

Estimation of the DDI risk between rivaroxaban and the three TKIs

According to the inhibition constants of the TKIs for CYP2J2- and CYP3A4-mediated rivaroxaban metabolism, the AUC fold-changes when the TKIs were combined with rivaroxaban were predicted. All predictions were performed based on the C_{max} of patients with solid tumours after administering recommended TKI doses (Gschwind et al., 2005; Scheffler, Di Gion, Doroshyenko, Wolf & Fuhr, 2011; Sparano et al., 2009). For patients with solid tumours, imatinib was predicted to influence rivaroxaban metabolism in vivo, leading to a 2.14–3.44-fold change in the AUC, which was predicted to result in a maximum rivaroxaban exposure increase of 244% (Table 6). Sunitinib and gefitinib were predicted to result in maximum rivaroxaban exposure increases of 2% and 11%, respectively.

Table 6. Prediction of drug interaction risk in vivo arising from inhibition of CYP2J2 and CYP3A4.

TKI	I (nM)[a]	AUC ratio[b]	AUC increase (%)
Imatinib	4,173–9,283	2.14–3.44	114–244
Sunitinib	62.99–69.52	1.02	2
Gefitinib	190.2–355.8	1.06–1.11	6–11

[a] I (μM) represents the C_{max} of patients with solid tumours, which were cited from (Di Gion et al., 2011; Gschwind et al., 2005; Sparano et al., 2009) for imatinib, (Di Gion et al., 2011) for sunitinib and (Scheffler, Di Gion, Doroshyenko, Wolf & Fuhr, 2011) for gefitinib.

[b] The AUC ratio was calculated based on Equations (2)–(4).

Discussion

There is extensive clinical application of rivaroxaban in combination with TKIs, and cancer patients are one of the main groups that receive rivaroxaban treatment. Due to the hypercoagulability of cancer patients and the thrombogenicity of anti-cancer agents, anticoagulant therapy has become an essential treatment for cancer patients. Increasing evidence has indicated that DOACs are safer and more convenient than classical anticoagulation medications, which is reflected in increasing clinical guidelines recommending that DOACs replace classical anticoagulation medications for cancer patient VTE therapy. In our previous study, CYP2J2, but not CYP3A4, was found to be dominant in the P450 metabolism of rivaroxaban with a contribution of 41.1%. However, few published reports have targeted CYP2J2 to explore the safety of rivaroxaban combinations, and even fewer of these have looked at rivaroxaban in combination with TKIs. Therefore, the estimation of DDI risk between TKIs and rivaroxaban based on CYP2J2 and CYP3A4 is necessary and meaningful for clinical practice. This was the focus of the present study.

All three TKIs were found to have a remarkable inhibitory effect on CYP3A4-mediated rivaroxaban metabolism. Imatinib showed the strongest reversible inhibitory effect towards CYP3A4 with a K_i value of 1.92 μM. The inhibition of CYP3A4 by sunitinib or gefitinib was also potent, with $K_i$values of 13.24 and 4.91 μM, respectively. In addition to reversible inhibition, the three TKIs also effected time-dependent inactivation of CYP3A4, especially sunitinib, which greatly increased the DDI risk in combination with rivaroxaban. Compared with reversible inhibition, mechanism-dependent inactivation is always more frequently related to unfavourable DDIs in clinical practice (Kalgutkar, Obach & Maurer, 2007). More importantly, the expression of CYP3A4—which is abundantly expressed P450 isoform in the liver in most individuals—showed more than 100-fold population variability (Zanger & Schwab, 2013). And meanwhile, it has been reported that sunitinib has a 10-fold higher concentration in the liver than in blood (Lau et al., 2015). Thus, being cautious about the CYP3A4 enzyme expression in patients who take both rivaroxaban and TKIs is necessary.

The present study found that CYP2J2, which dominates the metabolism of rivaroxaban, was inhibited by the TKIs. Notably, the three TKIs showed different inhibitory activity: imatinib and gefitinib were potent

Posted on 30 Jan 2024 — The copyright holder is the author/funder. All rights reserved. No reuse without permission. — https://doi.org/10.22541/au.170665457.70340859/v1 — This is a preprint and has not been peer-reviewed. Data may be preliminary.

inhibitors of CYP2J2 with K_i values of 3.53 and 2.99 μM, respectively, but sunitinib had almost no inhibitory effect on CYP2J2. Additionally, there was no irreversible inhibition of CYP2J2 by the three TKIs, with the results showing IC_{50} shifts of less than 1.5-fold. The basic principle of mechanism-based inactivation is the bioactivation of inhibitors, which is achieved by their metabolism by the inhibited enzymes (Kalgutkar, Obach & Maurer, 2007). Therefore, the results might suggest that the three TKIs were not or were rarely metabolised by CYP2J2.

Although the three TKIs did not irreversibly inactivate CYP2J2-mediated rivaroxaban metabolism, the DDI risk produced by inhibiting CYP2J2 cannot be ignored. The distribution of CYP2J2 in vivo is a potential factor that may increase the DDI risk of rivaroxaban in combination with TKIs. CYP2J2 was first detected in the liver but was since identified as an enzyme that is mainly distributed in the heart (Das, Weigle, Arnold, Kim, Carnevale & Huff, 2020); indeed, the mRNA levels of CYP2J2 in the cardiovascular system exceed those of other detected isozymes by 3 million to 62 times (Michaud, Frappier, Dumas & Turgeon, 2010; Wu, Moomaw, Tomer, Falck & Zeldin, 1996). Although CYP2J2 is not usually considered to be a DDI target due to its lower content in the liver, if the heart is set as the organ for potential DDIs, there may be an extremely high risk of DDI between rivaroxaban and TKIs.

In addition to its physiological distribution in the cardiovascular system, CYP2J2 has also recently been found to be highly expressed in various tumour tissues (Das, Weigle, Arnold, Kim, Carnevale & Huff, 2020; Jiang et al., 2005; Karkhanis, Hong & Chan, 2017). Due to the overexpression of receptors in tumours (such as PDGFR and EGFR), TKIs would accumulate in the tumour tissue. Therefore, the DDI risks of rivaroxaban in combination with TKIs for cancer patients may be higher than in our predictions, and CYP2J2 may need to become a target for DDI assessments involving rivaroxaban.

Imatinib was predicted to have moderate DDI risk when combined with rivaroxaban. Based on the inhibitory constants of imatinib on CYP2J2 and CYP3A4, and the metabolic contributions of two isoforms, imatinib was predicted to yield at most a 2.44-fold rivaroxaban AUC increase. Therefore, according to the FDA's guidelines for the relative risk of DDIs, a moderate DDI risk may exist for the combination of rivaroxaban and imatinib (Table 6). This result was predicted from the pharmacokinetic data of patients with solid tumours who were received TKIs. Notably, cancer patients have poorer metabolic function than normal patients, which may directly lead to higher plasma concentrations of TKIs for cancer patients. Therefore, using pharmacokinetic data from cancer patients may make our prediction more accurate. However, metabolic enzyme activity in the normal population is subject to individual variability, so factors such as hepatic blood flow and genetic polymorphism cannot be neglected (Zanger & Schwab, 2013). Factors that influence the enzyme activity of cancer patients may be more difficult to determine due to the more complicated in vivo environment. All these factors would affect the accuracy of our prediction in clinical practice. Additionally, the plasma concentrations of anti-cancer drugs in patients with solid tumours that are refractory to standard therapy are much higher than those of normal patients, which may result from large doses of anti-cancer drugs and metabolic function disorders (Scheffler, Di Gion, Doroshyenko, Wolf & Fuhr, 2011). Furthermore, it has been reported that lower plasma concentrations of TKIs (< 1100 ng·ml^{-1}) are closely related to the much faster development of progressive disease and lower objective response rates for GIST patients (von Mehren & Widmer, 2011). All these factors would produce great diversity in the pharmacokinetic data of TKIs in cancer patients. Thus, a rough in vitro prediction may neglect to indicate the risk of severe DDI in some individuals. Therefore, an individual physiologically-based pharmacokinetic model for cancer patients would be encouraged in the prediction of the pharmacokinetic behaviour of rivaroxaban in combination with TKIs.

In summary, all three TKIs (imatinib, sunitinib and gefitinib) showed inhibitory effects on CYP2J2- and CYP3A4-mediated rivaroxaban metabolism. Imatinib and gefitinib exerted significant reversible inhibition of CYP2J2 and CYP3A4, while sunitinib only showed reversible inhibition of CYP3A4. The three TKIs also demonstrated time-dependent inactivation of CYP3A4, with this effect being slight on CYP2J2. Furthermore, the combination of rivaroxaban with imatinib was predicted to constitute a moderate DDI risk. Our results provide data for the clinical safety assessment of the combination of rivaroxaban with imatinib, sunitinib

Posted on 30 Jan 2024 — The copyright holder is the author/funder. All rights reserved. No reuse without permission. — https://doi.org/10.22541/au.170665457.70340859/v1 — This is a preprint and has not been peer-reviewed. Data may be preliminary.

and gefitinib in cancer patients, and also give new insights for DDI assessment involving rivaroxaban.

Allison SE, Chen Y, Petrovic N, Zhang J, Bourget K, Mackenzie PI*, et al.* (2017). Activation of ALDH1A1 in MDA-MB-468 breast cancer cells that over-express CYP2J2 protects against paclitaxel-dependent cell death mediated by reactive oxygen species. Biochem Pharmacol 143**:** 79-89.

Blom JW, Doggen CJ, Osanto S, & Rosendaal FR (2005). Malignancies, prothrombotic mutations, and the risk of venous thrombosis. Jama 293**:** 715-722.

Burotto M, Manasanch EE, Wilkerson J, & Fojo T (2015). Gefitinib and erlotinib in metastatic non-small cell lung cancer: a meta-analysis of toxicity and efficacy of randomized clinical trials. Oncologist 20**:** 400-410.

Cheng AL, Kang YK, Lin DY, Park JW, Kudo M, Qin S*, et al.* (2013). Sunitinib versus sorafenib in advanced hepatocellular cancer: results of a randomized phase III trial. Journal of clinical oncology : official journal of the American Society of Clinical Oncology 31**:**4067-4075.

Cheong EJ, Goh JJ, Hong Y, Venkatesan G, Liu Y, Chiu GN*, et al.*(2017). Application of Static Modeling –in the Prediction of In Vivo Drug-Drug Interactions between Rivaroxaban and Antiarrhythmic Agents Based on In Vitro Inhibition Studies. Drug Metab Dispos 45**:**260-268.

Crusz SM, & Balkwill FR (2015). Inflammation and cancer: advances and new agents. Nat Rev Clin Oncol 12**:** 584-596.

Das A, Weigle AT, Arnold WR, Kim JS, Carnevale LN, & Huff HC (2020). CYP2J2 Molecular Recognition: A New Axis for Therapeutic Design. Pharmacol Ther 215**:** 107601.

Dhillon S (2015). Gefitinib: a review of its use in adults with advanced non-small cell lung cancer. Target Oncol 10**:** 153-170.

Di Gion P, Kanefendt F, Lindauer A, Scheffler M, Doroshyenko O, Fuhr U*, et al.* (2011). Clinical pharmacokinetics of tyrosine kinase inhibitors: focus on pyrimidines, pyridines and pyrroles. Clin Pharmacokinet 50**:** 551-603.

Diakos CI, Charles KA, McMillan DC, & Clarke SJ (2014). Cancer-related inflammation and treatment effectiveness. Lancet Oncol 15**:**e493-503.

Douketis JD, Crowther MA, Foster GA, & Ginsberg JS (2001). Does the location of thrombosis determine the risk of disease recurrence in patients with proximal deep vein thrombosis? Am J Med 110**:**515-519.

Fahmi OA, Maurer TS, Kish M, Cardenas E, Boldt S, & Nettleton D (2008). A combined model for predicting CYP3A4 clinical net drug-drug interaction based on CYP3A4 inhibition, inactivation, and induction determined in vitro. Drug Metab Dispos 36**:** 1698-1708.

Farmakis D, Parissis J, & Filippatos G (2014). Insights into onco-cardiology: atrial fibrillation in cancer. J Am Coll Cardiol 63**:** 945-953.

Gschwind HP, Pfaar U, Waldmeier F, Zollinger M, Sayer C, Zbinden P*, et al.* (2005). Metabolism and disposition of imatinib mesylate in healthy volunteers. Drug Metab Dispos 33**:** 1503-1512.

Guilhot F (2004). Indications for imatinib mesylate therapy and clinical management. Oncologist 9**:** 271-281.

Isoherranen N, Lutz JD, Chung SP, Hachad H, Levy RH, & Ragueneau-Majlessi I (2012). Importance of multi-p450 inhibition in drug-drug interactions: evaluation of incidence, inhibition magnitude, and prediction from in vitro data. Chem Res Toxicol 25**:**2285-2300.

January CT, Wann LS, Calkins H, Chen LY, Cigarroa JE, Cleveland JC, Jr.*, et al.* (2019). 2019 AHA/ACC/HRS Focused Update of the 2014 AHA/ACC/HRS Guideline for the Management of Patients With Atrial Fibrillation: A Report of the American College of Cardiology/American Heart Association Task Force on Clinical Practice Guidelines and the Heart Rhythm Society in Collaboration With the Society of Thoracic Surgeons. Circulation 140**:** e125-e151.

Posted on 30 Jan 2024 — The copyright holder is the author/funder. All rights reserved. No reuse without permission. — https://doi.org/10.22541/au.170665457.70340859/v1 — This is a preprint and has not been peer-reviewed. Data may be preliminary.

Jiang JG, Chen CL, Card JW, Yang S, Chen JX, Fu XN*, et al.*(2005). Cytochrome P450 2J2 promotes the neoplastic phenotype of carcinoma cells and is up-regulated in human tumors. Cancer Res 65**:** 4707-4715.

Jiao Q, Bi L, Ren Y, Song S, Wang Q, & Wang YS (2018). Advances in studies of tyrosine kinase inhibitors and their acquired resistance. Mol Cancer 17**:** 36.

Kalgutkar AS, Obach RS, & Maurer TS (2007). Mechanism-based inactivation of cytochrome P450 enzymes: chemical mechanisms, structure-activity relationships and relationship to clinical drug-drug interactions and idiosyncratic adverse drug reactions. Curr Drug Metab 8**:** 407-447.

Kalra S, Rini BI, & Jonasch E (2015). Alternate sunitinib schedules in patients with metastatic renal cell carcinoma. Ann Oncol 26**:**1300-1304.

Karkhanis A, Hong Y, & Chan ECY (2017). Inhibition and inactivation of human CYP2J2: Implications in cardiac pathophysiology and opportunities in cancer therapy. Biochem Pharmacol 135**:** 12-21.

Kuczynski EA, Lee CR, Man S, Chen E, & Kerbel RS (2015). Effects of Sorafenib Dose on Acquired Reversible Resistance and Toxicity in Hepatocellular Carcinoma. Cancer Res 75**:** 2510-2519.

Lau CL, Chan ST, Selvaratanam M, Khoo HW, Lim AY, Modamio P*, et al.* (2015). Sunitinib-ibuprofen drug interaction affects the pharmacokinetics and tissue distribution of sunitinib to brain, liver, and kidney in male and female mice differently. Fundamental & clinical pharmacology 29**:** 404-416.

Levitan N, Dowlati A, Remick SC, Tahsildar HI, Sivinski LD, Beyth R*, et al.* (1999). Rates of initial and recurrent thromboembolic disease among patients with malignancy versus those without malignancy. Risk analysis using Medicare claims data. Medicine (Baltimore) 78**:** 285-291.

Li JN, Cao YF, He RR, Ge GB, Guo B, & Wu JJ (2018). Evidence for Shikonin acting as an active inhibitor of human carboxylesterases 2: Implications for herb-drug combination. Phytother Res 32**:**1311-1319.

Michaud V, Frappier M, Dumas MC, & Turgeon J (2010). Metabolic activity and mRNA levels of human cardiac CYP450s involved in drug metabolism. PLoS One 5**:** e15666.

Monreal M, Falgá C, Valdés M, Suárez C, Gabriel F, Tolosa C*, et al.* (2006). Fatal pulmonary embolism and fatal bleeding in cancer patients with venous thromboembolism: findings from the RIETE registry. J Thromb Haemost 4**:** 1950-1956.

Nattel S, Burstein B, & Dobrev D (2008). Atrial remodeling and atrial fibrillation: mechanisms and implications. Circulation Arrhythmia and electrophysiology 1**:** 62-73.

Nattel S, & Harada M (2014). Atrial remodeling and atrial fibrillation: recent advances and translational perspectives. J Am Coll Cardiol 63**:** 2335-2345.

Nebot N, Crettol S, d'Esposito F, Tattam B, Hibbs DE, & Murray M (2010). Participation of CYP2C8 and CYP3A4 in the N-demethylation of imatinib in human hepatic microsomes. Br J Pharmacol 161**:**1059-1069.

Ning J, Liu T, Dong P, Wang W, Ge G, Wang B*, et al.* (2019). Molecular Design Strategy to Construct the Near-Infrared Fluorescent Probe for Selectively Sensing Human Cytochrome P450 2J2. J Am Chem Soc 141**:** 1126-1134.

O'Brien SG, Guilhot F, Larson RA, Gathmann I, Baccarani M, Cervantes F*, et al.* (2003). Imatinib compared with interferon and low-dose cytarabine for newly diagnosed chronic-phase chronic myeloid leukemia. N Engl J Med 348**:** 994-1004.

Onaitis M, D'Amico T, Zhao Y, O'Brien S, & Harpole D (2010). Risk factors for atrial fibrillation after lung cancer surgery: analysis of the Society of Thoracic Surgeons general thoracic surgery database. Ann Thorac Surg 90**:** 368-374.

Posted on 30 Jan 2024 — The copyright holder is the author/funder. All rights reserved. No reuse without permission. — https://doi.org/10.22541/au.170665457.70346859/v1 — This is a preprint and has not been peer-reviewed. Data may be preliminary.

Prandoni P, Lensing AW, Piccioli A, Bernardi E, Simioni P, Girolami B*, et al.* (2002). Recurrent venous thromboembolism and bleeding complications during anticoagulant treatment in patients with cancer and venous thrombosis. Blood 100**:** 3484-3488.

Prins MH, Lensing AW, Bauersachs R, van Bellen B, Bounameaux H, Brighton TA*, et al.* (2013). Oral rivaroxaban versus standard therapy for the treatment of symptomatic venous thromboembolism: a pooled analysis of the EINSTEIN-DVT and PE randomized studies. Thrombosis journal 11**:** 21.

Saliba W, Rennert HS, Gronich N, Gruber SB, & Rennert G (2018). Association of atrial fibrillation and cancer: Analysis from two large population-based case-control studies. PLoS One 13**:** e0190324.

Sanfilippo KM, & Wang TF (2019). Prevention and Treatment of Cancer-Associated Venous Thromboembolism: a Review. Curr Treat Options Cardiovasc Med 21**:** 70.

Scheffler M, Di Gion P, Doroshyenko O, Wolf J, & Fuhr U (2011). Clinical pharmacokinetics of tyrosine kinase inhibitors: focus on 4-anilinoquinazolines. Clin Pharmacokinet 50**:** 371-403.

Shalhoub J, Norrie J, Baker C, Bradbury AW, Dhillon K, Everington T*, et al.* (2017). Graduated Compression Stockings as an Adjunct to Low Dose Low Molecular Weight Heparin in Venous Thromboembolism Prevention in Surgery: A Multicentre Randomised Controlled Trial. Eur J Vasc Endovasc Surg 53**:** 880-885.

Song AB, Rosovsky RP, Connors JM, & Al-Samkari H (2019). Direct oral anticoagulants for treatment and prevention of venous thromboembolism in cancer patients. Vascular health and risk management 15**:**175-186.

Sparano BA, Egorin MJ, Parise RA, Walters J, Komazec KA, Redner RL*, et al.* (2009). Effect of antacid on imatinib absorption. Cancer Chemother Pharmacol 63**:** 525-528.

Streiff MB (2016). Thrombosis in the setting of cancer. Hematology Am Soc Hematol Educ Program 2016**:** 196-205.

Streiff MB, Holmstrom B, Angelini D, Ashrani A, Bockenstedt PL, Chesney C*, et al.* (2020). NCCN Guidelines Insights: Cancer-Associated Venous Thromboembolic Disease, Version 1.2020. J Natl Compr Canc Netw 16**:** 1289-1303.

Timp JF, Braekkan SK, Versteeg HH, & Cannegieter SC (2013). Epidemiology of cancer-associated venous thrombosis. Blood 122**:**1712-1723.

Tirumani SH, Jagannathan JP, Krajewski KM, Shinagare AB, Jacene H, & Ramaiya NH (2013). Imatinib and beyond in gastrointestinal stromal tumors: A radiologist's perspective. AJR Am J Roentgenol 201**:**801-810.

von Mehren M, & Widmer N (2011). Correlations between imatinib pharmacokinetics, pharmacodynamics, adherence, and clinical response in advanced metastatic gastrointestinal stromal tumor (GIST): an emerging role for drug blood level testing? Cancer Treat Rev 37**:**291-299.

Wertheimer C, Siedlecki J, Kook D, Mayer WJ, Wolf A, Klingenstein A*, et al.* (2015). EGFR inhibitor Gefitinib attenuates posterior capsule opacification in vitro and in the ex vivo human capsular bag model. Graefes Arch Clin Exp Ophthalmol 253**:** 409-417.

Wu S, Moomaw CR, Tomer KB, Falck JR, & Zeldin DC (1996). Molecular cloning and expression of CYP2J2, a human cytochrome P450 arachidonic acid epoxygenase highly expressed in heart. J Biol Chem 271**:**3460-3468.

Zamorano JL, Lancellotti P, Rodriguez Muñoz D, Aboyans V, Asteggiano R, Galderisi M*, et al.* (2016). 2016 ESC Position Paper on cancer treatments and cardiovascular toxicity developed under the auspices of the ESC Committee for Practice Guidelines: The Task Force for cancer treatments and cardiovascular toxicity of the European Society of Cardiology (ESC). Eur Heart J 37**:** 2768-2801.

Zanger UM, & Schwab M (2013). Cytochrome P450 enzymes in drug metabolism: regulation of gene expression, enzyme activities, and impact of genetic variation. Pharmacol Ther 138**:** 103-141.

Zhao T, Chen Y, Wang D, Wang L, Dong P, Zhao S*, et al.* (2021). Identifying the Dominant Contribution of Human Cytochrome P450 2J2 to the Metabolism of Rivaroxaban, an Oral Anticoagulant. Cardiovasc Drugs Ther.

Posted on 30 Jan 2024 — The copyright holder is the author/funder. All rights reserved. No reuse without permission. — https://doi.org/10.22541/au.170665457.70346859/v1 — This is a preprint and has not been peer-reviewed. Data may be preliminary.